# Qubit Energy-Relaxation Statistics in the Bluefors Quantum Measurement System

June 3, 2021

Slawomir Simbierowicz[1], Chunyan Shi[2], Michele Collodo[2], Moritz Kirste[2], Farid Hassani[3], Johannes Fink[3], Jonas Bylander[4], Daniel Perez Lozano[4], Russell Lake[1]

[1]Bluefors Quantum Team
[2]Zurich Instruments AG
[3]IST-Austria
[4]Chalmers University of Technology

BLUEFORS

# 1 Introduction

Superconducting qubits have emerged as a highly versatile and useful platform for quantum technological applications [1]. Bluefors and Zurich Instruments have supported the growth of this field from the 2010s onwards by providing well-engineered and reliable measurement infrastructure [2]– [6].

Having a long and stable qubit lifetime is a critical system property. Therefore, considerable effort has already gone into measuring qubit energy-relaxation timescales and their fluctuations, see Refs. [7]–[10] among others. Accurately extracting the statistics of a quantum device requires users to perform time consuming measurements. One measurement challenge is that the detection of the state-dependent response of a superconducting resonator due to a dispersively-coupled qubit requires an inherently low signal level. Consequently, measurements must be performed using a microwave probe that contains only a few microwave photons. Improving the signal-to-noise ratio (SNR) by using near-quantum limited parametric amplifiers as well as the use of optimized signal processing enabled by efficient room temperature instrumentation help to reduce measurement time. An empirical observation for fixed-frequency transmons from recent literature is that as the energy-relaxation time $T_1$ increases, so do its natural temporal fluctuations [7], [10]. This necessitates many repeated measurements to understand the statistics (see for example, Ref. [10]). In addition, as state-of-the-art qubits increase in lifetime, longer measurement times are expected to obtain accurate statistics. As described below, the scaling of the widths of the qubit energy-relaxation distributions also reveal clues about the origin of the energy-relaxation.

For the application of analyzing qubit energy-relaxation statistics, we utilize the Zurich Instruments Quantum Computing Control System in a Bluefors dilution refrigerator measurement system. We have measured three different fixed-frequency transmons at the Bluefors factory, including both 2D and 3D transmons. We characterize the statistics of qubit energy-relaxation time ($T_1$), and obtain mean values under typical operating conditions for measurement times of up to ~100 hours. In addition, we compare these measurements with results from another laboratory, and describe a model for the origins of qubit energy-relaxation fluctuations. This follows previous literature studies of decoherence benchmarking [7], and sets the stage for finding the root causes of environmentally induced energy-relaxation. Our methodology is enabled by the Zurich Instruments instrumentation which offers long-term stability, high SNR, low phase-noise, fast setup time, and ease of use.

# 2 Measurement

## 2.1 Bluefors and Zurich Instruments measurement setup

A previous application note on Superconducting Qubit Characterization summarizes the basic measurement procedure for frequency-tunable qubits. In the present application note, we follow a similar approach with the exception that the devices we measure are fixed-frequency transmons [11]. Figure 1 shows both the room temperature electronics and dilution refrigerator measurement system. The Zurich Instruments UHFQA Quantum Analyzer is used for qubit readout. The readout signal is generated by upconverting I and Q signals from the UHFQA with a microwave generator LO1 using an IQ mixer. The signal through a 2D or 3D cavity is then amplified and downconverted to I and Q signals at an intermediate frequency with the same microwave generator. After signal acquisition and data processing on the UHFQA, the measurement results are recorded and sent to a host computer. The qubit control signal is generated in a similar fashion, here I and Q pulses from the Zurich Instruments HDAWG multi-channel Arbitrary Waveform Generator are upconverted to the 4–8 GHz band with another microwave generator LO2 using the Zurich Instruments HDIQ IQ Modulator. The control and readout pulses are aligned via a trigger signal sent from the HDAWG to the UHFQA.

The coaxial wiring shown in Figure 1 comprises standard components from the Bluefors Coaxial Wiring catalog in an LD250 dilution refrigerator measurement system. The system has a base temperature of 10 mK with all coaxial wiring installed, and is equipped with a gold-plated copper radiation shield at the still flange. The system also employs the standard Bluefors wiring options including the Bluefors IR Filter, and cryogenic amplification and isolation.

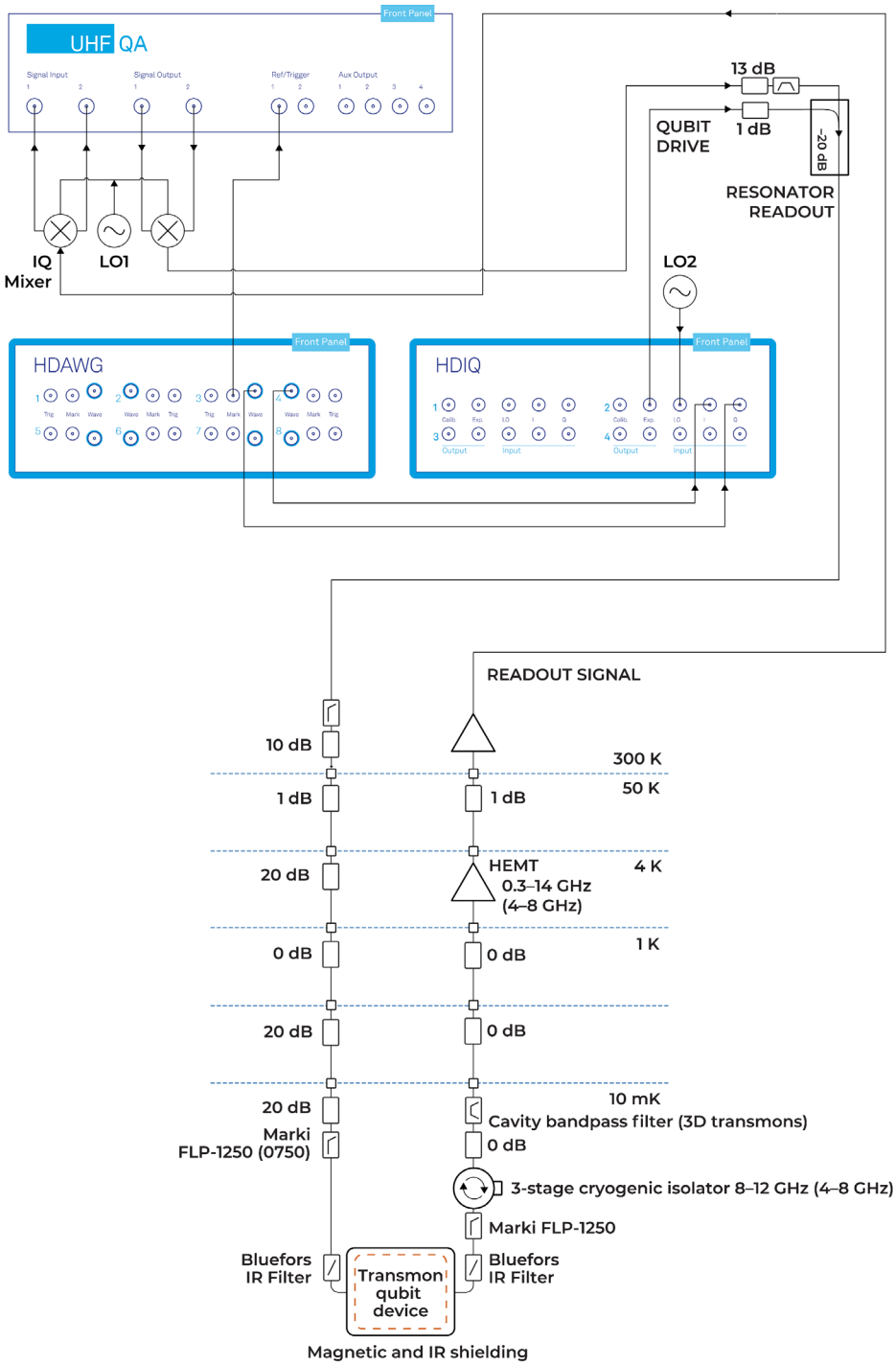


Figure 1: Quantum measurement system used to measure statistics of energy-relaxation time for fixed-frequency transmon qubit devices. Wiring was adjusted to perform measurements in bands around 6 GHz or 10 GHz.

## 2.2 Transmon device samples

We use transmon qubits to perform this investigation because they are widely employed for a variety of quantum measurements in the field. The sample type and operation frequencies of the samples used in these measurements are summarized in Table 1. Sample 1 was designed and fabricated at Chalmers University and is similar to what has been described previously by Burnett et al. [7]. Samples 2 and 3 are two nominally identical 3D transmon qubit devices designed and fabricated by the Fink Group at IST-Austria.

Table 1: Table of samples used for decoherence benchmarking in a typical LD250 default setup

| | **Sample type** | **Cavity frequency (GHz)** | **Qubit frequency (GHz)** | **Comment on wiring** |
|---|---|---|---|---|
| **Sample 1** | 2D | 6.03 | 3.79 | No IR filter on readout |
| **Sample 2** | 3D | 10.43 | 4.61 | As Fig. 1 |
| **Sample 3** | 3D | 10.44 | 4.45 | rf switch + 3 dB attenuator on sample input at 100 mK |

## 2.3 Data and statistical model

### 2.3.1 Data

To measure the energy-relaxation time of the qubit samples, we excite the qubit using a π-pulse and then measure the remaining population after a variable waiting time in averaged readout. $T_1$ is the exponential decay constant for relaxation from the excited state to the ground state of the qubit. We repeat many measurements of $T_1$ and plot the results in a time series across more than 30 hours for Samples 1 and 3 (Figure 2). The data points in Figure 2 were acquired in separate cooldowns. As described in Section 2.2, Samples 2 and 3 have a higher frequency readout resonator (~10 GHz), which necessitated changing room temperature microwave components, and cryogenic filters during the measurement runs. We note that the $T_1$ measurement repetition period is 3 minutes for Sample 1 and 4 minutes for Sample 3. The measurement repetition period for Sample 2 (not shown) is 11 minutes. These measurements comprise both 2D and 3D transmon qubits, see Table 1.

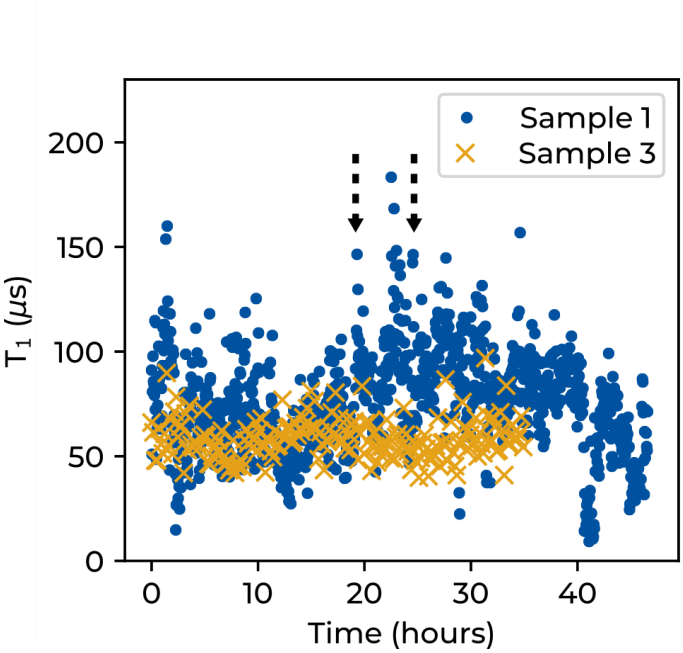


Figure 2: Time series of $T_1$ measurements for Sample 1 and Sample 3 (excerpt from full datasets). The samples were measured in different cooldowns. Arrows indicate where datasets have been concatenated for Sample 1.

The mean $\langle T_1 \rangle$ and the standard deviation $\sigma_{T_1}$ were extracted from all measurements of each sample, and the results are listed in Table 2. We plot $T_1$ histograms for all three samples measured at Bluefors in Figure 3. We also plot normal distributions in Figure 3 using the ($\langle T_1 \rangle$, $\sigma_{T_1}$) parameters extracted from each dataset and observe that the data are well described by a normal distribution. We conclude that the datasets are not dominated by rare processes that cause energy-relaxation at much shorter timescales

than $\langle T_1 \rangle$. However, Sample 2 does show a resolvable peak at 20 µs with a much smaller weight than the primary peak centered at $\langle T_1 \rangle$. In general, $T_1$ tends to vary symmetrically about its mean value.

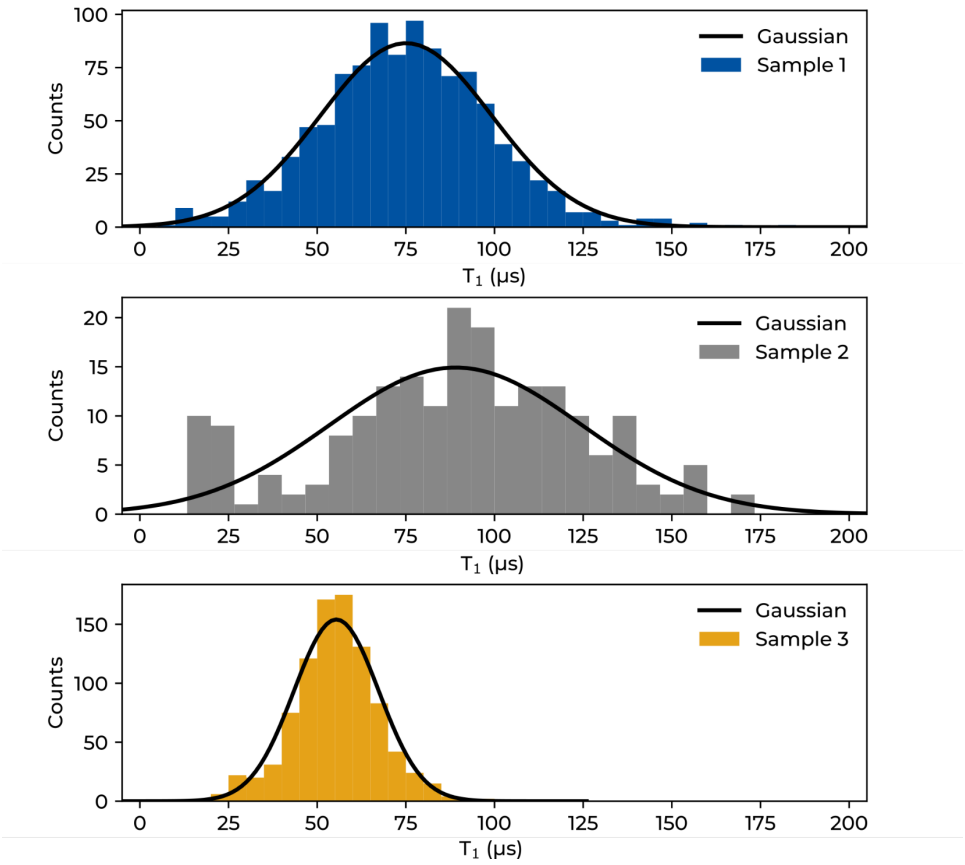


Figure 3: Histograms of $T_1$ measured at Bluefors for three samples. The number of measurements were $N_1$=1047, $N_2$=200, and $N_3$=924. The measurements span several hours to capture slow temporal variations in $T_1$.

Table 2: Summary of energy-relaxation statistics. "+" indicates a break between measurement runs. The relative errors of individual $T_1$ fits for Samples 1, 2, and 3 are 7 %, 5 %, and 7 % on average. The stated uncertainty is the standard error of $\langle T_1 \rangle$.

| | **Mean $\langle T_1 \rangle$ (µs)** | **Standard deviation $\sigma_{T_1}$ (µs)** | **Measurement time (h)** |
|---|---|---|---|
| **Sample 1** | 75 ± 0.7 | 24 | 19+5+22 |
| **Sample 2** | 89 ± 3 | 36 | 36 |
| **Sample 3** | 55 ± 0.4 | 12 | 14+35+24+18 |

## 2.3.2 Model and analysis

To gain insight into the origin of the energy-relaxation, we write down a model that relates the standard deviation of the measured qubit energy-relaxation time $\sigma_{T_1}$ to its mean value $\langle T_1 \rangle$. We follow an approach recently presented by Li et al. [10]. To model the data, we begin by considering $T_1$ as being limited by a population of thermally excited quasiparticles $N_{qp}$, or dissipative channels on the chip $N_C$,

$$T_1 = \frac{A}{N_C N_{qp}},$$

where *A* is a fitting pre-factor. We consider an ansatz where the dissipative channels that cause relaxation follow a Poisson distribution with width $\sigma_{N_C} = \sqrt{N_C}$. If the thermal quasiparticle population remains constant, the width of the distribution in the measured qubit lifetime is given by the relation

$$\sigma_{T_1} = |\partial T_1/\partial N_c|\, \sigma_{N_C}\,.$$

This leads to a well-defined prediction for the power law $\sigma_{T_1} \propto T_1^{3/2}$ if $T_1$ is limited by the intrinsic dissipative losses on the qubit chip (orange line in Figure 4). As described by Li et al., the degradation of qubit lifetime due to increasing temperature would follow a different power law due to an increasing population of thermal quasiparticles.

Figure 4 shows a brief survey of fixed-frequency transmon lifetime fluctuation statistics from Bluefors, and Chalmers University [7] in Bluefors dilution refrigerator systems. All measurements were acquired at a base temperature of approximately 10 mK. Blue circular markers are the data points from Table 1. The black crosses of Ref. [7] represent 2000 consecutive measurements over 65 hours.

We observe that the scaling results follow the same monotonically increasing trend but do not directly match the prediction for scaling governed by Poisson-distributed dissipative channels described by a simple $T_1^{3/2}$ power law. The apparent offset between the blue circular markers and black crosses may also reveal differences between measurement configurations. We also note that as qubit lifetimes improve, longer measurements are required to accurately capture the fluctuations in $T_1$ and determine the functional dependence of $\sigma_{T_1}$ and $\langle T_1 \rangle$.

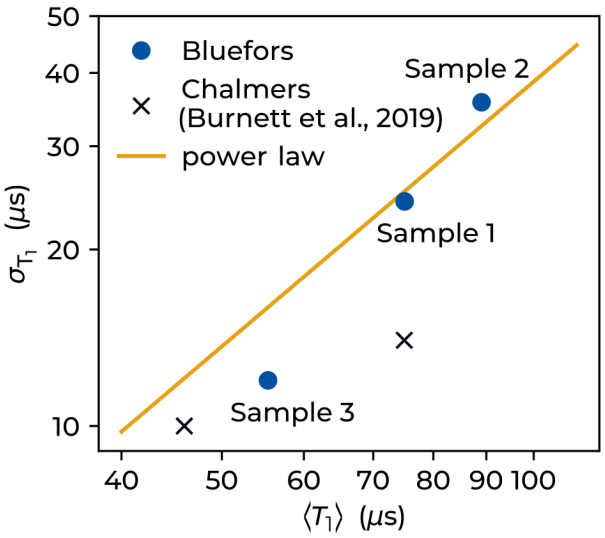


Figure 4: Mean $\langle T_1 \rangle$ plotted against the standard deviation $\sigma_{T_1}$ for various transmon qubits. Power law $\sigma_{T_1} \propto T_1^{3/2}$ is shown for reference

## 2.4 Phase coherence

In addition to the study of qubit lifetimes, we assess the coherence of Sample 1 by performing a Ramsey experiment comprised of two π/2 pulses separated by a variable time delay. Coherence measurements of superconducting qubits probe noise sources such as excess photons in the cavity [12]. For Sample 1, we measure a $T_1$ = 133 ± 10 µs and within 1 minute we perform a single Ramsey experiment. We extract $T_{2R}$ = 91 ± 9 µs which is in the regime of $T_{2R} < 2T_1$. This indicates that environmental noise may play a role in decoherence and its statistical properties may also reveal information about the noise source in future measurements. Further analysis of $T_2$ measurements can also reveal slow noise sources that cause decoherence [7].

# 3 Conclusions

In conclusion, we demonstrate that the Bluefors dilution refrigerator measurement system – when integrated with Zurich Instruments electronics – supports fast experimental implementation to enable long-time automatic measurements with high signal quality and low amplitude and phase noise. As a specific demonstration, we record histograms of qubit energy-relaxation times for timescales spanning up to 100 hours.

Primary conclusions based on these measurements can be summarized as follows. All transmon samples measured follow a normal-distribution of qubit lifetime fluctuations, i.e., the distributions are symmetric around the mean. Width of the distrubtions increase as qubit lifetime increases. The data do not directly follow a basic prediction for energy-relaxation limited by Poisson distributed dissipative channels $\sigma_{T_1} \propto T_1^{3/2}$, but the data measured at Bluefors in Figure 4 are consistent with a power law with an exponent greater than unity.

When combined with temperature-dependent data or a controllable noise source [13], the analysis of $T_1$ statistics will be a powerful tool to benchmark the physical infrastructure of superconducting qubit measurements. Ongoing work at Bluefors focuses on identifying the physical origins of the fluctuations in qubit energy-relaxation times to optimize our measurement systems. These kinds of measurements support the development of new integrated solutions that improve filtering, shielding, and protect qubits from environmental noise.

# 4 Contact

Email correspondence: Slawomir.Simbierowicz@bluefors.com, Russell.Lake@bluefors.com, Michele.Collodo@zhinst.com

# 5 References

[1] M. Kjaergaard, M. E. Schwartz, J. Braumüller, P. Krantz, J. I. J. Wang, S. Gustavsson and W. D. Oliver, “Superconducting Qubits: Current State of Play,” *Annual Review of Condensed Matter Physics,* vol. 11, p. 369, 2020.

[2] C. K. Andersen, A. Remm, S. Lazar, S. Krinner, N. Larcoix, G. J. Norris, M. Gabureac, C. Eichler and A. Wallraff, “Repeated quantum error detection in a surface code,” *Nature Physics,* vol. 16, pp. 875-880, 2020.

[3] A. Bengtsson, P. Vikstål, C. Warren, M. Svensson, X. Gu, A. F. Kockum, P. Krantz, C. Križan, D. Shiri, I. Svensson, G. Tancredi, G. Johansson, P. Delsing, G. Ferrini and J. Bylander, “Improved Success Probability with Greater Circuit Depth for the Quantum Approximate Optimization Algorithm,” *Physical Review Applied,* vol. 14, p. 034010, 2020.

[4] S. Krinner, S. Storz, P. Kurpiers, P. Magnard, J. Heinsoo, R. Keller, J. Lütolf, C. Eichler and A. Wallraff, “Engineering cryogenic setups for 100-qubit scale superconducting circuit systems,” *EPJ Quantum Technology,* vol. 6, p. 2, 2019.

[5] C. C. Bultink, B. Tarasinski, N. Haandbæk, S. Poletto, N. Haider, D. J. Michalak, A. Bruno and L. DiCarlo, “General method for extracting the quantum efficiency of dispersive qubit readout in circuit QED,” *Applied Physics Letters,* vol. 112, p. 092601, 2018.

[6] J. Heinsoo, C. K. Andersen, A. Remm, S. Krinner, T. Walter, Y. Salathé, S. Gasparinetti, J. Besse, A. Potočnik, A. Wallraff and C. Eichler, "Rapid High-fidelity Multiplexed Readout of Superconducting Qubits," *Physical Review Applied,* vol. 10, p. 034040, 2018.

[7] J. J. Burnett, A. Bengtsson, M. Scigliuzzo, D. Niepce, M. Kudra, P. Delsing and J. Bylander, "Decoherence benchmarking of superconducting qubits," *npj Quantum Information,* vol. 5, p. 54, 2019.

[8] P. Klimov, J. Kelly, Z. Chen, M. Neeley, A. Megrant, B. Burkett, R. Barends, K. Arya, B. Chiaro, Y. Chen, A. Dunsworth, A. Fowler, B. Foxen, C. Gidney, M. Giustina, R. Graff, T. Huang, E. Jeffrey, E. Lucero, J. Y. Mutus, O. Naaman, C. Neill, C. Quintana, P. Roushan, D. Sank, A. Vainsencher, J. Wenner, T. C. White, S. Boixo, R. Babbush, V. N. Smelyanskiy, H. Neven and J. M. Martinis, "Fluctuations of Energy-Relaxation Times in Superconducting Qubits," *Physical Review Letters,* vol. 121, p. 090502, 2019.

[9] S. Schlör, J. Lisenfeld, C. Müller, A. Bilmes, A. Schneider, D. P. Pappas, A. V. Ustinov and M. Weides, "Correlating Decoherence in Transmon Qubits: Low Frequency Noise by Single Fluctuators," *Physical Review Letters,* vol. 123, no. 190502, 2019.

[10] K. Li, S. Dutta, R. Zhang, Z. Steffen, D. Poppert, J. Bowser, S. Keshvari, B. Palmer, C. J. Lobb and F. C. Wellstood, "Large fluctuations of T1 in long-lived transmon qubits," in *APS March Meeting Epitome*, 2021.

[11] J. Koch, T. M. Yu, J. Gambetta, A. A. Houck, D. I. Schuster, J. Majer, A. Blais, M. H. Devoret, S. M. Girvin and R. J. Schoelkopf, "Charge-insensitive qubit design derived from the Cooper pair box," *Physical Review A,* vol. 76, p. 042319, 2007.

[12] C. Rigetti, J. M. Gambetta, S. Poletto, B. L. T. Plourde, J. M. Chow, A. D. Córcoles, J. A. Smolin, S. T. Merkel, J. R. Rozen, G. A. Keefe, M. B. Rothwell, M. B. Ketchen and M. Steffen, "Superconducting qubit in a waveguide cavity with a coherence time approaching 0.1 ms," *Physical Review B,* vol. 86, p. 100506(R), 2012.

[13] S. Simbierowicz, V. Vesterinen, J. Milem, A. Lintunen, M. Oksanen, L. Roschier, L. Grönberg, J. Hassel, D. Gunnarsson and R. E. Lake, "Characterizing cryogenic amplifiers with a matched temperature-variable noise source," *Review of Scientific Instruments,* vol. 92, p. 034708, 2021.